BWR Mechanics and Materials Technology Program Update

E. Kiss
Plant Materials and Mechanics Technology, General Electric Company,
175 Curtner Avenue, San Jose, California 95125, U.S.A.

Summary

This paper has discussed several varied and important technical activities being pursued at General Electric for the purpose of qualifying and improving BWR product technologies that fall broadly under the disciplines of Applied Mechanics and Materials Engineering. Each of these areas discussed are of general interest to the LWR industry although the focus of application is the Boiling Water Reactor. Specific results are reported for the areas of Dynamic Analysis and Modelling, Fatigue and Fracture Evaluation, Materials Advances, and Flow Induced Vibration.

Acknowledgement

The author gratefully acknowledges the contributions of the following members of the Plant Technology Section staff. Specifically, C.V. Subramanian, J.R. Fitch, H.S. Mehta, S. Ranganath, G.M. Gordon, P. Aldred, M.L. Herrera, D. Weinstein and B.M. Gordon

Introduction

This paper discusses technical results obtained from a variety of programs underway at the General Electric's Nuclear Engineering Division which deal with current technical issues that are of general importance to the LWR industry; albeit the specific focus is directed to the development and qualification of analytical predictive methods and criteria, and improved materials for use in the design of the Boiling Water Reactor (BWR). Specific results and accomplishments are summarized to provide a broad perspective of technology advances.

1. Dynamic Analysis and Modeling

1.1 Standard Plant Soil-Structure Interaction Evaluation

A previous paper (Reference 1) discussed in detail the approach taken by General Electric for the design of a standard BWR Nuclear Steam Supply System (NSSS). An important part of such an evaluation is the soil-structure interaction (SSI) analysis methodology. Historically, SSI analysis of nuclear power plants has been performed using both compliance and finite element methodologies. Since it was not generally possible to decide à-priori on which approach was superior, an evaluation was undertaken using the GE standard BWR Nuclear Island (STRIDE) to provide a consistent comparison of SSI methodologies. Results are described herein.

The finite element approach utilizing the FLUSH Computer Code is described in detail in Reference 2. The compliance method utilized employs the half space model and computer code CLASSI (Reference 3). Figure 1 shows the reactor building and reactor pressure vessel model with comparison node points identified. The results focus on four specific soil-site cases. Three are for 75 ft soil depth and one at 150 ft depth. Four soil stiffnesses were considered, ranging from soft to hard rock as characterized by shear wave velocities ranging from 1000 ft/sec to 3500 ft/sec. Evaluations were consistent with applicable U.S. NRC regulatory guides and the input control motion was applied in the free field at the finished grade depth.

A comparison of maximum accelerations and moments for the two methods is given in Table A and for several locations in the plant. Figure 2 shows comparison of a typical response spectra. In general, this study shows that the finite element approach predicts plant responses which are higher than the compliance method approach in the frequency range of prime importance to reactor equipment design (>5 Hz). The largest difference was noted for the softer soil case. One factor believed to contribute to the lower SSI results using the compliance approach is the larger rocking predicted. Depending on phasing the rotational effect can significantly influence the horizontal input motion.

1.2 Coupled Structural Fluid Interaction Analysis

A new method for defining the SRV air-clearing load and for calculating the response of a pressure suppression containment structure has been developed. The method differs in two respects from previous approaches in which a prescribed pressure loading (obtained from direct measurement) is applied to the containment walls. First, the suppression pool fluid and the oscillating air bubbles are explicitly simulated in the

mathematical model. Secondly, the excitation of the system is enforced at the interface between the air bubbles and the surrounding fluid.

An axisymmetric model of the bubble-fluid-structure system is used to illustrate the application of this method. Modelling considerations included the load definition and containment response calculations which are based on the assumption that the SRV air bubble oscillation can be simulated by a linear acoustic model. The problem is idealized by postulating that the air bubble exists in equilibrium with the surrounding fluid at the initial time. A key assumption* is that the time duration for initial compression and expulsion of air is short relative to that of the resulting pressure oscillation. The short-duration forcing function is applied to the bubble surface and the bubble begins to oscillate. Numerical solution of the problem is achieved by means of coupled finite-element modelling of the containment structure, suppression pool water, and air bubble using a General Electric computer code developed from the NASTRAN Code (Reference 4).

Figure 3 shows a pressure history and amplified response spectrum measured during SRV testing in a relatively rigid wall test facility. The dominant frequency is between 7 and 8 Hz and the amplitude attenuation is equivalent to a damping of about 7.5% of critical. To simulate the short duration initial transient, a bubble forcing function was derived in the form of a pulse-like excitation which is applied over a time period of about 40 milli-seconds. The amplitude of the pulse and the modal damping were chosen to match the peak pressures and attenuation of the test trace. Applying the derived forcing function to the model in which the suppression pool fluid is coupled to the containment shell shows the predicted pressure on the base mat is still dominated by the 7 Hz oscillation. However, a dramatically different situation is seen in Figure 4 which shows the pressure at the flexible containment wall. The containment wall pressure is dominated by an 18 Hz signal which corresponds to the fundamental coupled breathing mode of the containment shell and the suppression pool.

The major feature of the method described herein is that it can be used to realistically predict the dynamic response of the coupled system due to the SRV discharge transients. By modelling the bubble and exciting it with a pulse, the energy input to the coupled system is realistically bounded such that artificial predicted resonances resulting from applying the pressures directly as a wall load force, are avoided.

2. Fatigue and Fracture Evaluation

The following sections discuss the development of the fracture diagram, a key element required to assess the structural margin of cracked piping components. The second section discusses the weld nugget technique for analyzing the resulting residual stress in welded pipe joints and compares the resulting analysis and experimental data.

2.1 Fracture Diagram "Leak-vs-Break"

For many LWR components made of high strength materials, the critical crack size, and hence structural margin, is typically determined on the basis of linear elastic fracture

*This assumption is based on experimental observations in laboratory tests and at several operating plants.

mechanics (LEFM) methods. However, for piping components made of materials which exhibit high ductility in operation, such as stainless steel, failure is characterized by extensive yielding and subsequent plastic instability. For such ductile behavior the net-section collapse method has been developed and used to determine the critical crack sizes in piping. Application has focused on the part-through and through-wall circumferential cracks since this was most consistent with observed field cracking in welded piping.

The net-section collapse approach assumes that a flawed pipe is at the point of incipient failure when the net-section in the cracked plane forms a plastic hinge. The methodology is discussed in (Reference 5). This approach has been shown to be effective in predicting failure of stainless steel pipes containing circumferential cracks (Reference 6) and was further benchmarked by comparisons with the experimental data and currently available elastic-plastic fracture methods. Figure 5 shows a fracture analysis diagram developed for stainless steel piping. The stress level shown corresponds to a combination of primary (8 ksi) and bending (16 ksi) equal to the ASME Code limit of 1.5 S_m. Stress due to thermal gradients and differential expansion need not be included since secondary stresses do not affect the net-section collapse load.

The fracture analysis diagram shows that stainless steel pipes can tolerate large circumferential cracks without failure. For example, even at the uncracked stress level of 1.5 S_m, a 360^o circumferential crack extending through 50% of the wall thickness is not expected to break. Examination of available field data for circumferential cracks in.2 inch to 10 inch diameter austenitic pipes provides additional assurance weld zone cracks will grow through-wall to leak before the collapse load is reached. This "leak-before-break" tendency has been shown to be consistent for large pipes susceptible to stress corrosion cracking.

The net-section collapse method is currently under consideration for adoption by the ASME Section XI - "In-Service Inspection Code for Nuclear Plant Components." This will allow a straightforward quantitative assessment of design margin of cracked piping and serve as a rational technical basis for continued plant operation and effective plant in-service inspection.

2.2 Nugget Area Method For Weld Residual Stress Analysis

Extensive work has been done at General Electric in developing analytical methods for the determination of residual stresses in piping. Such models have typically been based on the moving point heat source assumption for temperature distributions. Since the accuracy of the predicted stress depends strongly on the assumed temperature, predictions have been made using an improved thermal model for welding referred to as the Nugget Area Heating Method (NAH). This method assumes that the weld nugget remains at the melting temperature for a finite period of time followed by conduction cooling. The size of the weld nugget and the duration of heating are based on experimental observations (Reference 8).

Using the nugget area temperature, a transient heat transfer analysis is performed. The temperatures are then used as input for the elastic-plastic stress analysis (Reference 7). Elastic-plastic behavior based on the von Mises yield criterion and the Prandtl-Reuss equation is used. Subsequent yielding is evaluated using a kinematic hardening model. Sufficient number of steps are used to adequately represent the welding process. The residual stress is produced once the pipe has cooled to its initial stress free temperature.

Figure 6 shows the calculated tensile weld residual axial and hoop stress on the inside surface of a 4 inch Schedule 80 pipe. The stresses and trends compare reasonably well with experimental measurements obtained in the laboratory (Reference 5). This type of analysis has been used in analyzing processes which can mitigate IGSCC in piping; such as Induction Heating Stress Improvement* (IHSI) which creates a favorable compressive residual stress in the HAZ of welded stainless steel piping (Reference 9). Figure 6 also shows the calculated residual stress following the IHSI process. Note that the high tensile stress on the pipe I.D. has been replaced with a compressive stress.

3. Materials Engineering Advances

3.1 Stress Corrosion Cracking Remedies

Development of qualified stress corrosion cracking remedies for welded stainless steel piping depends on two major factors. The first is the fundamental understanding of the cause of cracking, while the second is the ability to demonstrate and quantify improvement or immunity in the laboratory. Figure 7 shows that three ingredients must be simultaneously present for IGSCC of austenitic materials to occur. First, the material must be sufficiently sensitized by the welding process; second, there must be over yield stress; and thirdly, a sufficiently oxidizing (or conducive) environment must be present. If one or more of these conditions are removed, stress corrosion cracking will not occur.

The principle solution to pipe cracking in the BWR is the conversion to nuclear grade stainless steels. The fundamental difference between regular grade and nuclear grade is the carbon control at 0.02% maximum and the higher nitrogen ($\sim$.1%) to retain strength. To illustrate the excellent IGSCC resistance of 316 NG under accelerated laboratory conditions in GE's specialized Pipe Test Laboratory (PTL), Figure 8 shows a photomicrograph of a 304 stainless steel pipe that cracked after 2 years in service, the same material in PTL after 100 hours and a typical 316 NG welded pipe after >2000 hours in service. The absence of IGSCC after 2000 hours in PTL is equivalent to more than 40 years in service.

While the use of nuclear grade materials is considered the principle remedy, various other remedy options have been qualified. These are identified as follows: solution anneal; corrosion resistant cladding, heat sink welding, HISI and Hydrogen Water Chemistry.

Each of the remedies identified has been or is currently undergoing qualification in GE's PTL. In most cases, funding from EPRI and a BWR Owners Group was provided to support programs aimed at qualifying solutions to IGSCC of stainless steel piping.

3.2 Improved Fatigue Rules for Carbon Steel Components

While successful field experience with carbon steel components in the past has shown that the ASME Code fatigue analysis procedures are adequate, there are limiting conditions involving a combination of severe environment, high mean stress and notch effects, in which the Code fatigue design margins are reduced.

In order to evaluate these effects, a detailed experimental and analytical program on the fatigue behavior of carbon steel in high temperature water environment was established. The study included fatigue tests involving a wide variety of parameters such as water

*IHSI technique was first introduced by I.H.I. Company of Japan

environment, temperature, stress level, notch configuration and cyclic frequency. In addition to small specimen tests, fatigue tests were also run on welded pipes to simulate actual component behavior. In many of the tests, cracking appeared to be associated with notches or discontinuities.

The results show (Figure 9) that specific factors are required to account for butt weld fatigue strength reduction (K_f), environment (K_{en}), notches (K_n) and mean stress (K_m) in those cases where these parameters are sufficiently severe. Reference 10 provides detailed discussion of the four new factors shown in Equation I, developed to specifically account for these effects in a typical ASME fatigue analysis.

$$S_p = \frac{1}{2}(K_f K_n K_m K_{en}) K_e S_n \qquad [I]$$

Re-evaluation of the fatigue test data utilizing the appropriate corrections is shown in Figure 9 along with the ASME design curve. It is seen that except for one test point, the re-evaluated data fall above the ASME Code design curve. This implies that the current ASME design curve is adequate but that in those special cases where pipe butt welds are subjected to high mean stress in an oxygenated environment, specific evaluation of these effects must be considered in design to assure sufficient design margin.

4. Flow Induced Vibration

Since the late 1970's Flow Induced Vibration studies have focused on testing and evaluation of full-size prototype reactor internal components in General Electric's High Flow Hydraulic Facility. Utilizing the high flow capacity (~40,000 gpm) of this facility, FIV design margins have been quantified for all major BWR reactor internals, at flow rates significantly exceeding design rating. In addition, special investigations of simulated fuel bundles have been performed to further develop the fundamental understanding and technology related to the effects of flow rate, fluid temperature and two-phase flow on the FIV response of rods in parallel flow. A summary of recent test results is presented herein.

4.1 Test Description

A specially designed 3x3 fuel bundle was tested in GE's ATLAS Test Facility. All rods were full length, filled with simulated final pellets (tungsten carbide) to match the actual fuel rod mass, contained prototype spacer springs and end supports, and were contained in an appropriate flow channel. In all tests, the central rod was instrumented at various axial locations using bi-axial accelerometers encased in the rods.

Two basic types of flow tests were performed. The first included single-phase and two-phase inlet adiabatic flow. In the former, only temperature was varied while for the latter the inlet quality was varied as well. The second type of test utilized electrical resistance heating of the rods to produce boiling of the inlet water and to simulate the flow rates of a typical average power BWR bundle (scaled down to a nine rod bundle). A uniform power shape was used in these tests.

4.2 Testing Conditions

Single-phase tests were run at fluid temperatures of 180°F, 350°F, and 550°F at flow rates ranging from 50% to 150% of rated. Two-phase inlet steam-water flow tests were performed with inlet quality ranging from 5 to 20% and mass flux rates to 150% rated.

Boiling tests were run at bundle average powers corresponding to 150% rated.

4.3 Vibration Response

Rod vibration response is reported as the maximum rms value of the combined bi-axial acceleration measured along the rod length. The maximum response typically occurred above mid span. Figure 10 is a summary of maximum measured rod response in single phase, two-phase inlet, and boiling test conditions as a function of bundle mass flow rate. All curves shown are the result of a polynomial fit of the data.

Examination of Figure 10 shows a relatively small rms amplitude dependence on single-phase flow rate, with the lower temperature fluid producing higher excitation. However, in two-phase inlet and boiling tests there appears to be a competition between higher exit quality and mass flow rates such that the vibration amplitude tends to reach a peak value then decrease. This behavior has been previously reported in Reference 11. In general, however, rod vibration response was low level (≈.001 inch) broad band; e.g., 40 to 100 Hz and decreasing above 100 Hz.

TABLE A. COMPARISON OF SSI METHODS

MAXIMUM ACCELERATION RESPONSE (ft/sec^2)

Node Number	CASE 1 (1000 ft/sec)		CASE 2 (1500)		CASE 3 (2000)		CASE 4* (3500)	
	FE	CS	FE	CS	FE	CS	FE	CS
1	17.9	6.61	18.15	13.89	32.5	21.1	20.4	10.86
22	13.50	6.24	17.19	11.22	19.7	19.7	31.1	9.18
42	10.20	5.10	12.56	9.73	23.4	15.2	12.9	7.59
105	11.20	4.86	13.44	8.67	17.60	17.64	19.8	6.93

*150 Ft Depth

MAXIMUM MOMENTS ($x10^6$ ft-lbs)

Element Number	CASE 1		CASE 2		CASE 3		CASE 4*	
	FE	CS	FE	CS	FE	CS	FE	CS
41	1525	691	1614	1382	2774	1953	1787	1090
55	1027	420	953	778	1791	1197	897	619
70	59.7	42.1	71.8	75.0	96.4	106	89.7	60.5
101	4.70	1.85	6.05	3.69	7.57	7.01	7.66	2.72

Note: FE = Finite Element
CS = Compliance Spring

References

[1] KISS, E., GERBER, T. L., "Status of BWR Structural Integrity Programs at General Electric Company," Nuclear Engineering and Design, Vol. 59, No. 1, August 14, 1979.

[2] LYSMER, J., UDAKA, T., CTSAI, HSEED, "FLUSH--A Computer Program For Approximately Three-Dimensional Analysis of Soil-Structure-Interaction Problems," EERC 75-30, November 1975, University of California, Berkeley.

[3] WONG, H. L., LUCO, J. E., "The Application of Standard Finite Element Programs in the Analysis of Soil-Structure Interaction," Second SAP Users Conference, University of Southern California, Los Angeles, June 1977.

[4] MACNEAL, R. H., CITERLY, R. L., CHARGIN, M. K., "A New Method for Analyzing Fluid Structure Interaction Using NASTRAN," Trans. 5th SMiRT Conference, Vol. 8, August 1979.

[5] HORN, R. M., "The Growth and Stability of Stress Corrosion Cracks in Large Diameter Piping," EPRI Report NP-2472, July 1982.

[6] RANGANATH, S., MEHTA, H., "Engineering Methods for the Assessment of Ductile Fracture Margin in Nuclear Power Plant Piping," 2nd Symposium on Elastic-Plastic Fracture Mechanics, ASTM, October 6-9, 1981.

[7] ANSYS Engineering Analysis System, Swanson Systems, Inc., March 1975.

[8] "Last Pass Heat Sink Welding," Semi-Annual Report to EPRI, NEDC-22153-1 (October 1981 - April 1982).

[9] HERRERA, M. L., LANGE, C., RANGANATH, S., "Analytical Evaluation of Residual Stresses in Piping Subjected to IHSI," ASME 81-PVP-19.

[10] RANGANATH, S., et al, "Fatigue Behavior of Carbon Steel Components in High Temperature Water Environments," ASTM STP 770, pgs. 436-459.

[11] GORMAN, D. J., "Investigation of the Vibration of Cylindrical Reactor Fuel Elements in Two-Phase Parallel Flow," Nucl. Sci. Engr., 1971.

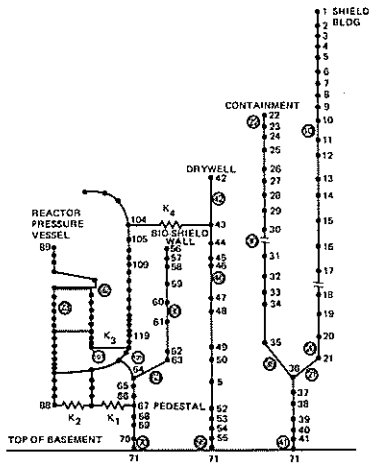

Figure 1 Building and Reactor Pressure Vessel Model

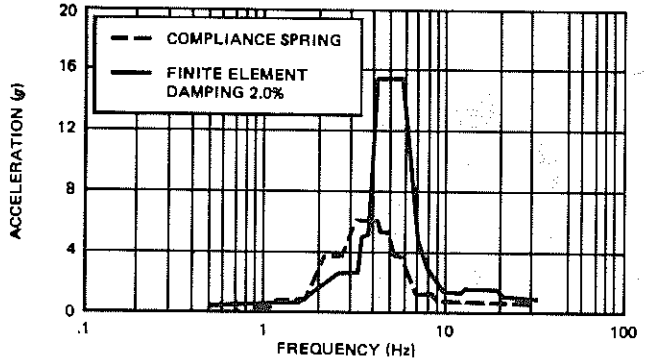

Figure 2. Comparison of Response Spectra at Node Point 1

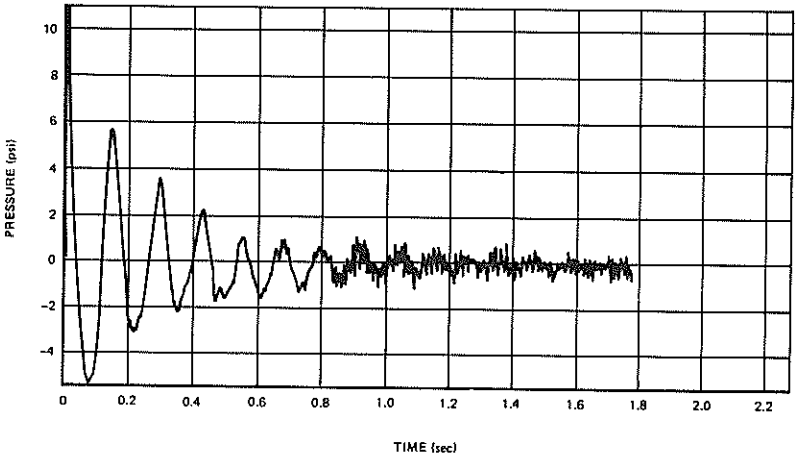

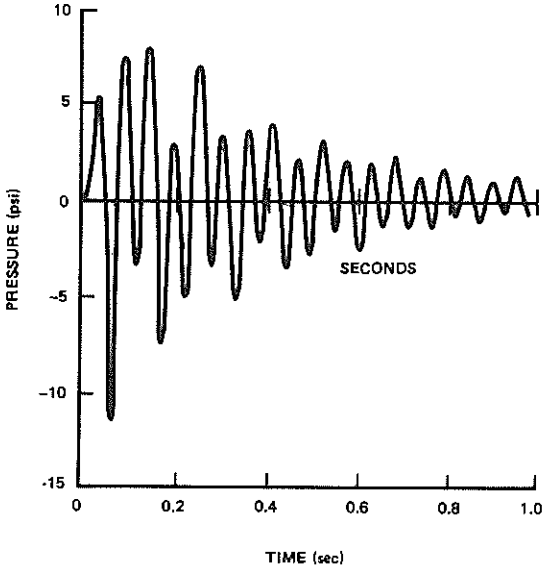

Figure 4. Pressure on Containment Wall Flexible-Wall Calculation

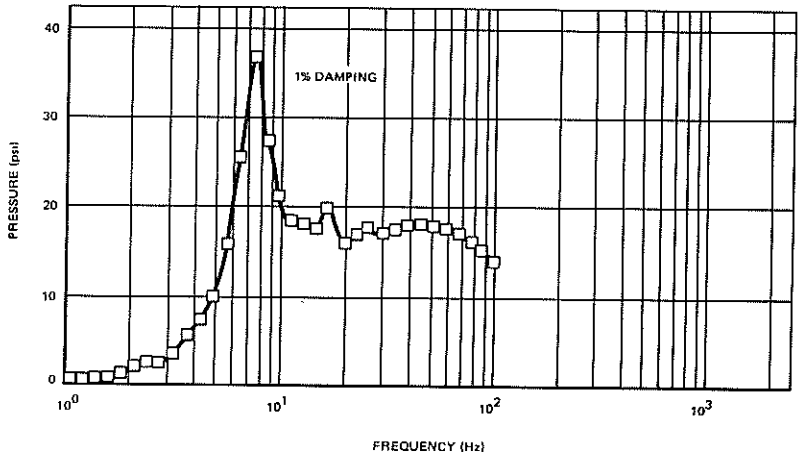

Figure 3. Measured Pressure History and Amplitude Response Spectrum

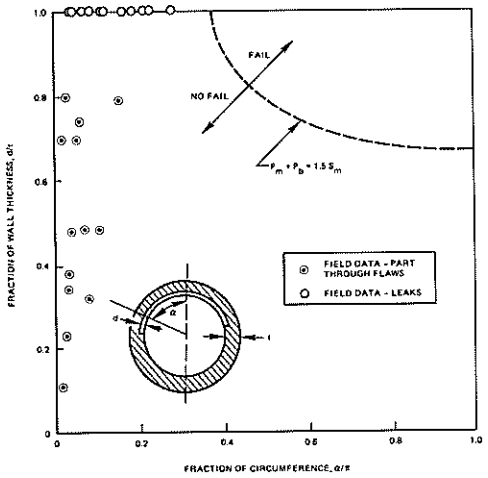

Figure 5. Fracture Analysis Diagram-Stainless Steel Piping

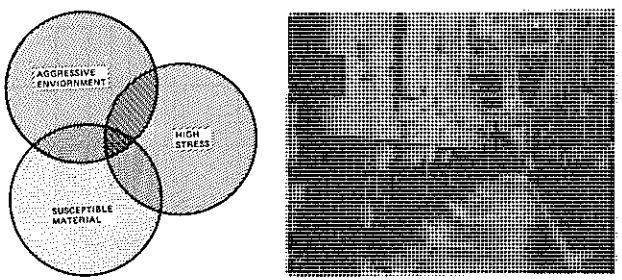

Figure 7. *General Electric Pipe Test Laboratory*

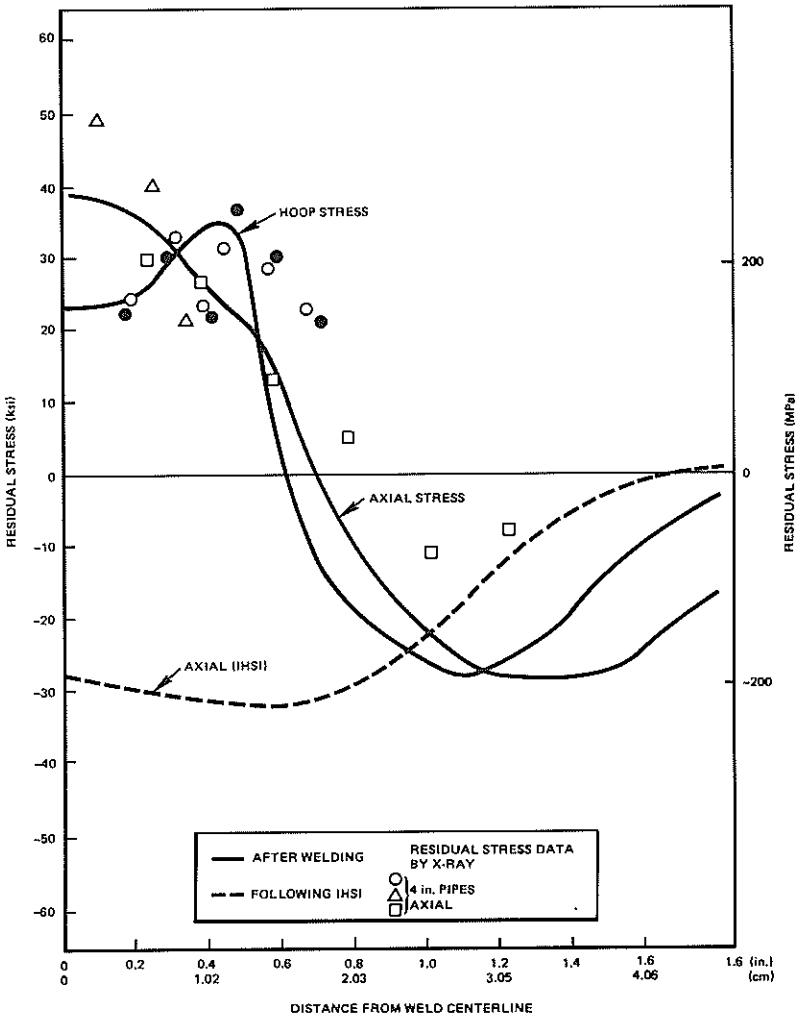

Figure 6. Residual Axial and Hoop Stress on Pipe I.D

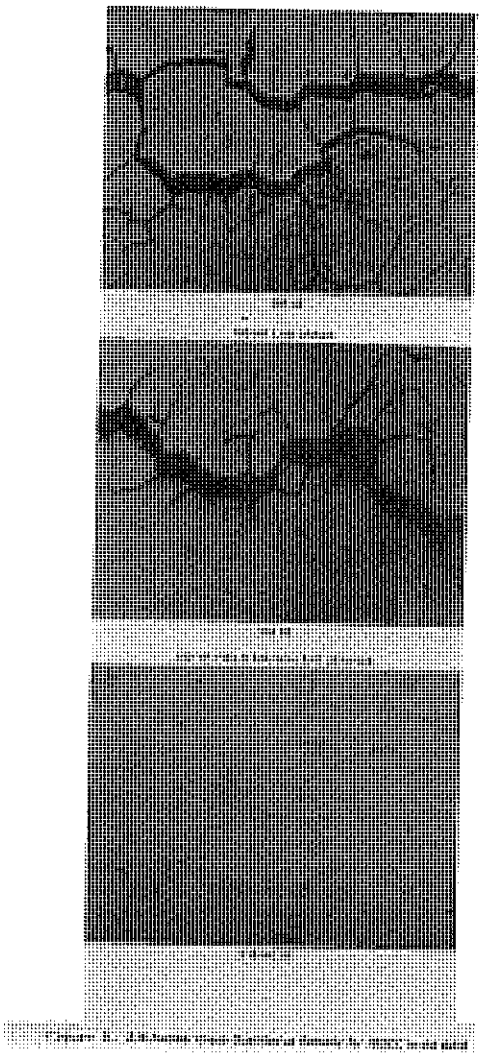

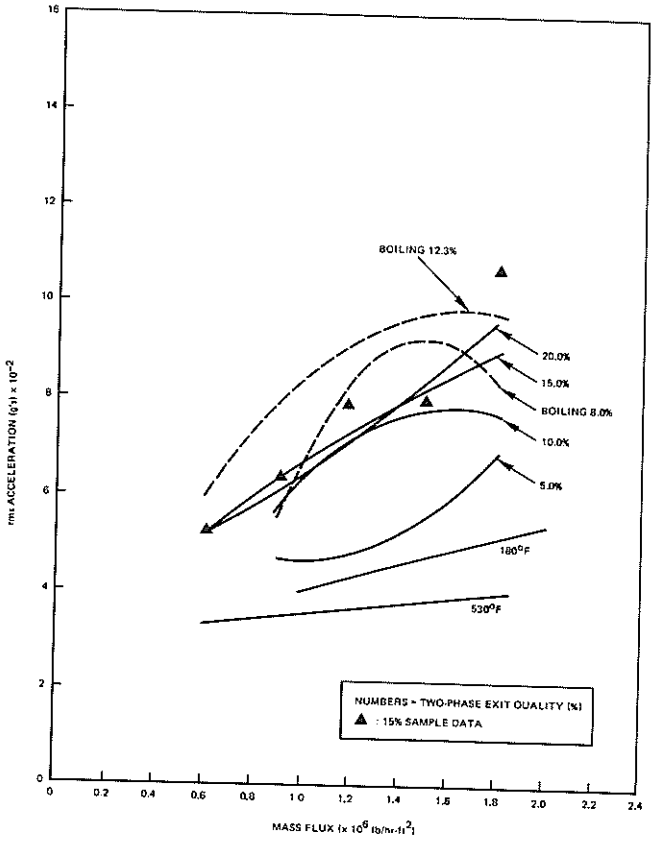

Figure 10. Rod Vibration Response

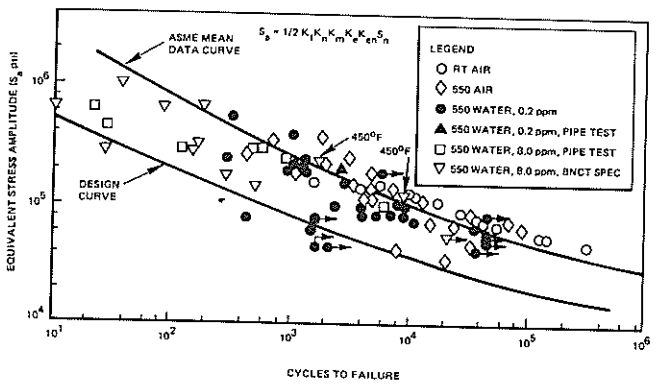

Figure 9. Test Results Evaluated by Proposed Rules

G 1/1*